ISSN 0853-2982 eISSN 2549-2659

JURNAL TEKNIK SIPIL

Jurnal Teoretis dan Terapan Bidang Rekayasa Sipil

# Higher-Order Finite Difference Scheme With Tvd Filter Algorithm Part 1: Simulations Of Scalar Advective Dominant Problems

**Muhammad Cahyono**

Faculty of Civil and Environmental Engineering, Institute of Technology Bandung, Jalan Ganesha 10, Bandung 40132, Indonesia Email : cahyono@itb.ac.id

**Abstract**

*Engquist et al. (1989) proposed non-linear TVD filters. When combined with a traditional higher-order finite difference scheme, these filters can simulate shock or high concentration gradient problems with no spurious oscillations. Among the filter proposed is the filter algorithm 2.2. However, this algorithm flattens extrema that are not the results of overshooting and consequency the scheme reduces to a low order of accuracy locally around smooth extrema. Modification of the TVD filter algorithm 2.2 has been applied in this paper to overcome this problem. Several conservative finite difference schemes are considered for testing the TVD filter. Non-conservative schemes consisting of 4th and 6th -order Runge-Kutta method are also evaluated. The modified filter has been tested to simulate seven test cases, including a pure advection of scalar profiles, a pure advection with variable velocity, two inviscid burger equations, an advection-diffusion equation with variable velocity and dispersion, advection of three solid bodies in rotating fluid around a square of a side length of 2, and a two-dimensional advection-diffusion equation. The numerical experiments showed that applying the modified TVD filter, combined with the higher-order non-TVD finite difference schemes for solving the advection equation, can produce accurate solutions with no oscillations and no clipping effect extrema.*

**Keywords :** Non-Oscillatory schemes, TVD filter, advection, higher-order accurate

**Abstrak**

*Engquist dkk. (1989) mengusulkan filter TVD non-linear. Ketika dikombinasikan dengan skema beda hingga orde tinggi tradisional, filter ini dapat mensimulasikan kejutan atau masalah gradien konsentrasi tinggi tanpa osilasi palsu. Di antara filter yang diusulkan adalah algoritma filter 2.2. Namun, algoritma ini meratakan ekstrem yang bukan merupakan hasil dari "overshooting" dan konsekuensinya skema tersebut direduksi ke tingkat akurasi yang rendah secara lokal di sekitar ekstrem halus. Modifikasi algoritma filter TVD 2.2 telah digunkan dalam makalah ini untuk mengatasi masalah ini. Beberapa skema konservatif dipertimbangkan untuk menguji filter TVD. Skema non-konservatif metode Runge-Kutta orde ke-4 dan ke-6 juga dievaluasi. Filter yang dimodifikasi diuji untuk mensimulasikan tujuh kasus, termasuk adveksi murni profil skalar, adveksi murni dengan kecepatan bervariasi, dua persamaan burger inviscid, persamaan adveksi-difusi dengan kecepatan bervariasi dan dispersi, adveksi tiga benda padat berputar oleh aliran di bidang persegi dengan panjang sisi 2, dan persamaan adveksi-difusi dua dimensi. Eksperimen numerik menunjukkan bahwa penerapan filter TVD yang dimodifikasi, dikombinasikan dengan skema beda hingga non-TVD orde tinggi untuk menyelesaikan persamaan adveksi, dapat menghasilkan solusi yang akurat tanpa osilasi dan tanpa efek kliping.*

**Kata Kunci :** Skema tanpa osilasi, Filter TVD, advection, orde-akurasi tinggi

## 1. Introduction

This paper proposes an application of a TVD filter algorithm to approximate equations of advective dominant problem. Firstly, we consider a one-dimensional advection problem defined by the hyperbolic conservative of **Equation (1)**.

$$\frac{\partial \emptyset}{\partial t} = \frac{\partial F(\emptyset)}{\partial x} \tag{1}$$

$$\emptyset(x,0) = u_0(x)$$

The hyperbolic conservation **Equation (1)** models a wide range of physically exciting phenomena such as advection of contaminants and sediments, shallow water flow, gas dynamics, etc. Obtaining an accurate approximation of the advection **Equation (1)** is challenging. Two of the issues that arise are the problems of oscillations or overshoots and undershoots and artificial diffusions. The application of traditional schemes such as second-order central, third-order QUICKEST (Leonard, 1979), and other higher-order schemes to approximate the advection **Equation (1)** has significant difficulties when discontinuities or sharp gradients are present in the solution (Deng et al., 2019). The schemes will generally produce spurious oscillations near these discontinuities or sharp gradients (Deng et al., 2019). The sharp numerical discontinuities can be reproduced without oscillations by applying high-resolution schemes such as the Total Variation Diminishing (TVD)-type schemes (Shu, 1988; Deng,et al., 2019), essentially non-oscillatory



Diterima 7 Juli 2022, Direvisi 28 Juli 2022, Diterima untuk dipublikasikan 11 Agustus 2022

(ENO) types of schemes (Su and Kim, 2018; Ha,et al., 2019), weighted essentially non-oscillatory (WENO) schemes (Liu and Qiu, 2016; Christlieb et al.,2019; Rajput and Singh, 2022), a series of hybrid WENO/central difference methods (Kim and Kwon, 2005), Limiter numerical fluxes schemes using the normalized variable formulation (Leonard, 1988; Leonard and Mohktari, 1990;-Gao et al., 2012; Zhang et al., 2021), the Godunov-type schemes with artificial viscosity—(Rodionov, 2017) and so on. The methods attempt to capture the discontinuity, generally known as the shock capture schemes. The sock capture schemes attempt to avoid spurious oscillations across sharp gradients and discontinuities while maintaining high-order accuracy in smooth extrema (Deng et al., 2019). These schemes are based on concepts like up winding, local Reiman solvers, field by field decomposition using polynomial interpolating for cell interface reconstruction, and flux limiting (Engquist et al., 1989). However, the algorithm proposed for these high-resolution schemes is quite complicated for higher-order numerical accuracy (Engquist et al., 1989).

To overcome these difficulties, more than three decades ago, Engquist et al. (1989) proposed an algorithm with non-linear filters, which, when combined with traditional schemes, can treat shocks and contact discontinues similarly to the modern high-resolution schemes. The filter was developed based on field-by-field decomposition similar to the non-oscillatory schemes and limiter to have good capturing high gradient or discontinuities. It is only activated at a few grid points where oscillations are detected. The filter maintains the order of accuracy and computationally efficiency close to the traditional methods (Engquist et al., (1989) . The filter has other advantages, they can be applied to the non-conservative schemes, and its time step is essentially independent of the step of the basic different scheme.

Engquist et al. (1989) proposed several TVD filters ranging from relatively simple algorithms 2.1 and 2.2 for one-dimensional hyperbolic equations to somewhat more complex algorithms, algorithm 4.1, to be applied to systems of hyperbolic equations. The filter evaluated in this study is the TVD filter algorithm 2.2. This filtering algorithm, combined with the higher-order finite difference scheme, has been used for solving the advection equation problems. The original algorithm 2.2 was modified to more accurately capture the true extrema and produce accurate solutions for long-term simulations. We consider several finite difference schemes for testing the TVD filter, including conservative based schemes such as second-order Lax-Wendroff, third-order QUICKEST (Leonard,1979), 4th and 6th -order conservative schemes (Leonard, 1988; 1991; Leonard and Mokhtari, 1990), and non-conservative schemes consisting of 5th and 6th -order accurate in space and using the 4th-order Runge-Kutta method for time integration. Only the last two schemes are described in this paper, while the other schemes for interested readers can look at the reference cited. Seven test cases were considered to gain insight into the merit of the TVD filter algorithm. These test cases include a pure advection of scalar profiles, a pure advection with variable velocity, two inviscid burger equations, an advection-diffusion equation with variable velocity and dispersion, advection of three solid bodies in rotating fluid around a square of a side length of 2, and a two-dimensional advection-diffusion equation. The resulting tests show that the modified TVD filter algorithm combined with the higher-order scheme can produce highly accurate results for solving the advection dominates problem with no oscillations. The following section describes the TVD algorithm, Runge-Kutta schemes, numerical testings, and conclusions.

## 2. Higher-Order Runge-Kutta Method

Time integration of **Eq. (1)** over time from t = t to t + Δt gives the following **Equation (2)**

$$\emptyset_j^{n+1} = \emptyset_j^n + \int_{t^n}^{t^{n+1}} \frac{\partial F(\emptyset)_i}{\partial x}\, dt \tag{2}$$

Gradient $\partial F(\phi)_i/\partial x$ can be approximated by using the 4th and 6th -order finite difference central scheme defined by **Equations (3)** and **(4)**.

$$\frac{\partial F(\emptyset)}{\partial x} = \frac{F_{i-2} - 8F_{i-1} + 8F_{i+1} - F_{i+2}}{12\,\Delta x} \tag{3}$$

$$\frac{\partial F(\emptyset)}{\partial x} = \frac{-F_{i-3} + 9F_{i-2} - 45F_{i-1} + 45F_{i+1} - 9F_{i+2} + F_{i+3}}{60\,\Delta x} \tag{4}$$

Integrating **Equation (2)** using 4th-order Runge-Kutta gives **Equations (5. a)** to **(5. e)**.

$$\phi_j^{n+1} = \phi_j^n + \frac{1}{6}(k_1 + 2k_2 + 2k_3 + k_4) \tag{5.a}$$

where

$$k_1 = \frac{\partial F(t^n, \phi_i^n)}{\partial x} = G(t^n, \phi^n) \tag{5.b}$$

$$k_2 = G(t^n + \Delta t/2, \phi^n + k_1\Delta t/2) \tag{5.c}$$

$$k_3 = G(t^n + \Delta t/2, \phi^n + k_2\Delta t/2) \tag{5.d}$$

$$k_4 = G(t^n + \Delta t, \phi^n + k_3\Delta t) \tag{5.e}$$

## 3. TVD Filter Algorithm

### 3.1 Original TVD algorithm

Assuming that $v_i^{n+1} = \varphi_i^{n+1}$ are the results after taking one step with a difference scheme which produces oscillations solutions, where $\varphi_i^n$ = value of ϕ at a grid point i at time level t = nΔt with Δt = time step. We denote two finite difference operators, namely $\Delta^+ v_j = v_{j+1} - v_j$ *and* $\Delta^- v_j = v_j - v_{j-1}$ . Engquist et al. (1989) proposed the following algorithm 2.1 (using the exact name of an algorithm used in the original paper) to eliminate oscillations.

**Algorithm 2.1** (Engquist et al., 1989)
**For** j:= 2 to N-1 **do**
  **If** $(\Delta^+ v_j^{n+1})(\Delta^- v_j^{n+1}) < 0$ **then**
    **If** $|\Delta^+ v_j^{n+1}| > |\Delta^- v_j^{n+1}|$ **then**



Diterima 7 Juli 2022, Direvisi 28 Juli 2022, Diterima untuk dipublikasikan 11 Agustus 2022

$\delta^+ := |\Delta^- v_j^{n+1}|$

$\delta^- := |\Delta^- v_j^{n+1}|$

**jcoor := j + 1**

**else**

$\delta^+ := |\Delta^- v_j^{n+1}|$

$\delta^- := |\Delta^+ v_j^{n+1}|$

**jcoor := j – 1**

**endif**

$\delta := min(\delta^-, \delta^+/_2)$

$s := sgn(\Delta^+ v_j^{n+1})$

$v_j^{n+1} := v_j^{n+1} + s\delta$

$v_{jcorr}^{n+1} := v_{jcorr}^{n+1} - s\delta$

**endif**

**endfor**

**Algorithm 2.1** is not entirely satisfactory due to:

1. Extrema consisting of more than one point cannot be detected,
2. TVD properties cannot be guaranteed, thus allowing oscillations present in the solution.
3. It flattens true extrema, the value that is not the result of overshooting, and thus produces a low order of accuracy locally around smooth extrema.

To overcome these disadvantages the algorithm 2.1 is modified using the algorithm 2.2 as follows.

**Algorithm 2.2** (Engquist et al., 1989)

J := 2

**While** j < N **do**

If $(\Delta^+ v_j^{n+1})(\Delta^- v_j^{n+1}) < 0$ and not admissible1 $(j, v^{n+1}, v^n) < 0$ **then**

Correct $v_j^{n+1}$ in the same way as in Algorithm 2.1.

**else if** $(\Delta^+ v_j^{n+1})(\Delta^- v_j^{n+1}) < 0$ and $(\Delta^+ v_{j-1}^{n+1})(\Delta^- v_{j-1}^{n+1}) < 0$ **then**

comment: this removes a zig-zag situation

$\delta := min(|\Delta^- v_{j-1}^{n+1}|, |\Delta^+ v_{j-1}^{n+1}|/2, |\Delta^+ v_j^{n+1}|)$

$s := sgn(\Delta^+ v_j^{n+1})$

$v_{j-1}^{n+1} := v_{j-1}^{n+1} - s\delta$

$v_j^{n+1} := v_j^{n+1} + s\delta$

$j := j - 1$

**else**

comment: if $v_j^{n+1}$ does not need any correction go on to j + 1

**endwhile**

The admissible1 $(j, v^{n+1}, v^n)$ function returns true if $min(v_{j-1}^n, v_j^n, v_{j+1}^n) < v_j^{n+1} < max(v_{j-1}^n, v_j^n, v_{j+1}^n)$ otherwise, the value false is returned. When we allow the case where there is a minimum at j-1 and a maximum at j, an additional function, admissible2 $(j, j-1, v^n, v^{n+1})$ must be introduced into the "else if" text in Algorithm 2.2, resulting in the new conditions:

elseif $(\Delta_j^+ v_j^{n+1})(\Delta^- v_j^{n+1}) < 0$ and $(\Delta_{j-1}^+ v_{j-1}^{n+1})(\Delta^- v_{j-1}^{n+1}) < 0$

and not admissible2 $(j, j-1, v^n, v^{n+1})$ then.

The admissible2 $(j, j-1, v^n, v^{n+1})$ function returns true if the following condition

$min(v_j^n, v_j^n) < v_j^{n+1} < max(v_j^n, v_{j+1}^n)$ and

$min(v_{j-2}^n, v_{j-1}^n, v_j^n) < v_{j-1}^{n+1} < max(v_{j-2}^n, v_{j-1}^n, v_j^n)$ or

$min(v_{j-1}^n, v_j^n, v_{j+1}^n) < v_j^{n+1} < max(v_{j-1}^n, v_j^n, v_{j+1}^n)$ and

$min(v_{j-2}^n, v_{j-1}^n) < v_{j-1}^{n+1} < max(v_{j-2}^n, v_{j-1}^n)$ hold.

Otherwise, the result is false. The algorithm 2.2 requires that the solution $v^n$ from previous time level has been saved.

### 3.2 Modification of TVD filter algorithm

As can be seen in the following numerical tests, the use of the TVD filter algorithm 2.2 (i.e., a modified form of the TVD filter algorithm 2.1) still gives results with the true extremum flattened and thus produce un-accurate results for a long terms simulation. It indicates that the admissible1 function fails to detect the actual extremum point properly. However, the filter is relatively simple and promising for application. The filter can achieve improvement by modifying the admissible1 function (Cahyono, 2000). The following section describes changing the admissible1 routine to capture the true extremum correctly (Cahyono, 2000). Therefore, the TVD filter algorithm 2.2 can be exactly relaxed at this point. Consequently, the true extremum was allowed to accentuate occasionally without the necessity to damp it out.

The modified admissible1 function, later called the admissible1_m function, assumes that the data have no sudden gradient change at or near the true extremum. The admissible1_m function detects the true extremum by the following algorithm.

**Function admissible1_m** (j,$n^{n+1}$,$n^n$)

If $(\Delta^+ v_j^{n+1}.\Delta^- v_j^{n+1}) < 0$ then

**If** $(\Delta^+ v_{j-1}^{n+1}.\Delta^- v_{j-1}^{n+1} > 0$ and $(\Delta^+ v_{j+1}^{n+1}.\Delta^- v_{j+1}^{n+1} > 0$ **then**

**If** $(|\Delta^+ v_j^{n+1}| < |\Delta^+ v_{j+1}^{n+1}|$ and $(|\Delta^- v_j^{n+1}| < |\Delta^- v_{j-1}^{n+1}|$ **then**

admissible1_m = 1

**else**

admissible1_m = 0

**endif**

**else**

admissible1_m = 0

**endif**

**else**



Diterima 7 Juli 2022, Direvisi 28 Juli 2022, Diterima untuk dipublikasikan 11 Agustus 2022

admissible1_m = 1

**endif**
return (admissible1_m)

The admissible1_m function is true (i.e., it detects the true extremum) when it returns unity; otherwise, it is false if it returns zero. The admissible1_m expressed in the above algorithm is similar to the Leonard-Niknafs discriminator (see Leonard and Niknafs, 1991), used for the same purpose. However, the former is more easily applied than the latter since the admissible1_m function needs only five cell stencils compared to the Leonard-Niknafs discriminator, which requires seven.

## 4. Numerical Test

### 4.1 Test 1. advection complex profiles

The first test considered is the advection of scalar profiles (i.e., solute concentration profiles) by the flow with a constant velocity, $a_o$,= 1 defined by **Eq. (6)**.

$$\frac{\partial \emptyset}{\partial t} + \frac{\partial (u_o)}{\partial x} = 0 \qquad (6)$$

The initial condition is given by **Eq. (7)**.The initial condition consists of four scalar profiles: narrow Gaussian distribution, a square wave, a triangle wave, and a semi-ellipse profile. These four profiles have several essential features. For example, the square wave profile shows the effect of spurious oscillations near discontinuities. The semi-ellipse profile shows the effect of terracing due to changes in the gradient involving a combination of sudden and gradual and. The narrow Gaussian and the triangle profiles show the effect of clipping at the extrema. The exact solution at time t is the initial profile translated by a distance $a_o$.t without shape change.

This sample test is usually employed to verify non-oscillatory type and shock-capturing schemes to evaluate their non-oscillatory property and numerical dissipation (Deng et al., 2019; Zhang et al., 2021). This test case was also considered in previous studies by Su and Kim (2018), Huang and Chen (2018), and Liu et al. (2018), Christlieb et al., (2019), Deng et al., (2019), and Ha and Lee (2020). However, they generally considered the problem for short-term simulations, i.e., T ≤ 1000 periods. In the present work, the study focuses on evaluating the performance of the TVD filter on several finite difference schemes in simulations starting from short periods T = 2 and 10, medium periods t = 100, to long periods t = 1000, 2000 5000. We use a periodic boundary condition (Christlieb et al., 2019). The calculation is performed using N = 400 cells with $C_r = U_o\ \Delta t/\Delta x = 0.4$. Simulations are carried out using the original filter algorithm 2,2 and its modified version. We use the abbreviation of schemes simulated using original filter algorithm 2.2 by LWOF2, QOF2, FLOF2, SLOF2, RK4OF2, and RK6OF2 schemes for Lax-Wendroff, Quickest (Leonard, 1979), the 5th, and 6th-order conservative schemes (Leonard, 1991), and the 4th and 6th-order Runge-Kutta schemes defined by Eq. (2) to (5), respectively. The corresponding names for the methods simulated using the modified filter are LWMF2, QMF2, FLMF2, SLMF2, RK4MF2, and RK6MF2. We also consider bound verse of the 6th-order (ULTIMATE) conservative schemes (Leonard, 1991), USL, for comparisons.

All simulation results are shown in **Figure 1** to **4**. The simulation results for t = 2, 10, 100, and 1000 using the original filter algorithm 2.2 are given in **Figure 1**, and those using the modified algorithm 2.2 are shown in **Figure 2**. It is seen that the simulation uses the original algorithms 2.2. produce reasonably accurate results at t = 2 and 10, but there is an initial profiles distortion and continuously worsens the solution quality for the period t = 100 and 1000. These show that the original filter algorithm 2.2 fails to produce accurate results for long-term simulations for t greater than 100. On the contrary, except for LWMF2, the use of the modified algorithm 2.2 can provide reasonably accurate results for long-term simulation at t = 1000, particularly for higher-order schemes such as FLMF2, SLMF2, RK4MF2, and RK6MF2 schemes. The clipping effect of Gaussian peaks and triangles is reduced in these higher-order schemes

The second-order LWMF2 produced inaccurate results for all periods considered. The TVD filter algorithm 2.2 failed to work at the Lax-Wendroff scheme. **Figure 3** shows the simulation results at t = 2000 and 5000 for FLMF2, SLMF2, RK4MF2, and RK6MF2. The FLMF2, SLMF2, and RK4MF2 failed to capture the peak of the initial profile, while the RK6MF2 was still able to capture the Gaussian and triangular profile shapes but failed to capture the rectangle and semi-ellipse profiles. **Figure 4.a** shows the comparison between FLMF2 and RK4MF2, and **Figure 4.b** between RK6MF2 and the USL. The RK4MF2 produces a more accurate solution than FLMF2 (see **Figure 4.a**), and The RK6MF2 can still capture Gaussian and triangular profiles. In contrast, the USL can capture rectangle and semi-ellipse profiles.

$$\emptyset_0(x) = \begin{cases} \frac{1}{6}\{g(x,\omega,z-\delta) + g(x,\omega,z+\delta) + 4g(x,\omega,z)\} & if -0.8 < x \le -0.6, \\ 1 & if -0.4 < x \le -0.2, \\ 1 - |10(x-0.1)| & if\ 0 < x \le 0.2, \\ \frac{1}{6}\{h(x,\vartheta,\alpha-\delta) + h(x,\vartheta,\alpha+\delta) + 4h(x,\vartheta,\alpha)\} & if\ 0.4 < x \le 0.6, \\ 0 & otherwise. \end{cases} \qquad (7)$$

Where $h(x,\vartheta,\alpha) = \sqrt{\max[1 - \vartheta^2\,(x-\alpha)^2, 0]}$

$\alpha = 0.5, \quad z = -0.7, \quad \delta = 0.005, \vartheta = 10, \ \omega = \frac{log\ 2}{36\ \delta^2}$ , and $g(x,\omega,z-\delta) = e^{-\omega(x-z)^2}$



Diterima 7 Juli 2022, Direvisi 28 Juli 2022, Diterima untuk dipublikasikan 11 Agustus 2022

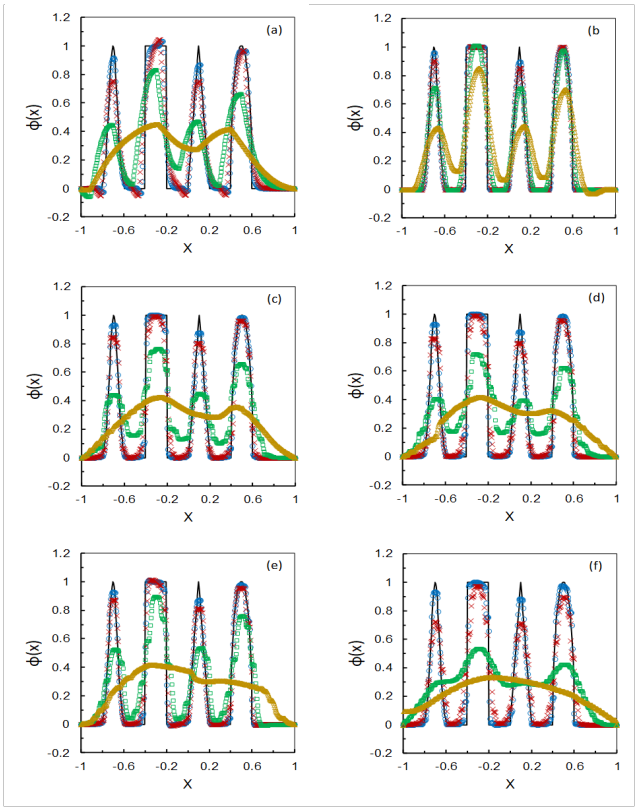


**Figure 1. Comparison of exact solutions with numerical solutions of Eq. (6) using original TVD algorithm 2.2 at t = 2 (blue circle O), 10 (red cross (x), 100 (green rectangle □), and 1000 (orange triangle Δ) for (a). LWOF2, (b). QOF2, (c). FLOF2, (d). SLOF2 , (e).RK4OF2 and (f). RK6OF2 schemes, respectively.**

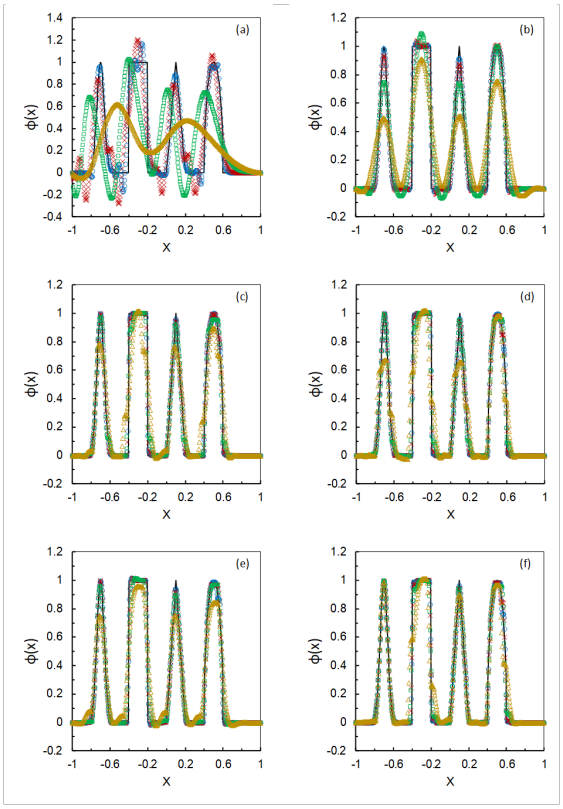


**Figure 2. Comparison of exact solutions with numerical solutions of Eq. (6) using modified TVD algorithm 2.2 at t = 2 (blue circle O), 10 (red cross (x), 100 (green rectangle □), and 1000 (orange triangle Δ) for (a). LWMF2, (b). QMF2, (c). FLMF2, (d). SLMF2, (e).RK4MF2 and (f). RK6MF2 schemes, respectively.**

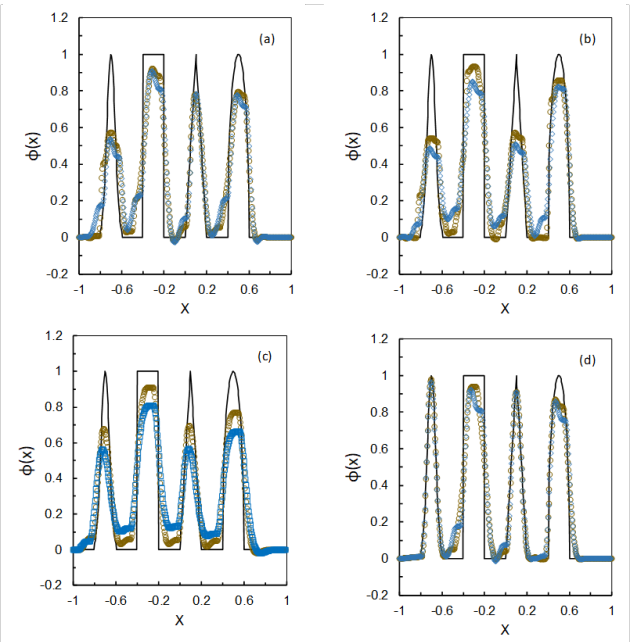


**Figure 3. Comparison of exact solution with numerical solution of Eq. (6) using modified TVD algorithm 2.2 at t = 2000 (brown circle O ) and 5000 (blue diamond ◊) for (a). FLMF2, (b). SLMF2, (c). RK4MF2, and (d). RK6MF2 schemes, respectively.**

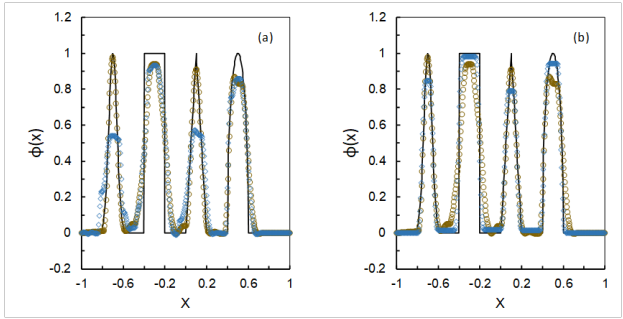


**Figure 4. Comparison of exact solution with numerical solution of Eq. (6) using modified TVD algorithm 2.2 at t = 5000 for (a). RK4MF2 (brown circle O ) and FLMF2 (blue diamond ◊)and (b). RK6MF2 (orange circle O) and Ultimate Sixth order (blue diamond ◊).**

The ability of the numerical model to capture the profile shape can be evaluated using the Nash-Sutcliffe efficiency coefficient, NSE, (Nash and Sutcliffe, 1970), defined by **Eq. (8)**.

$$NSE = 1 - \frac{\sum_{t=1}^{t=N}\left(\emptyset_{est,n} - \emptyset_{a,n}\right)^2}{\sum_{t=1}^{t=N}\left(\emptyset_{a,n} - \emptyset_{a,ave}\right)^2} \quad (8)$$

Where $\varphi_a$ and $\varphi_{est}$ are the numerical and exact value at node n, respectively, $\varphi_{a,ave}$ is the average of the exact value. The NSE value indicates whether the actual



Diterima 7 Juli 2022, Direvisi 28 Juli 2022, Diterima untuk dipublikasikan 11 Agustus 2022

**Table 1. NSE values for several schemes considered for simulation results at t = 1000 and 2000 for profiles Gaussian (A), triangle (B), and semi-ellipse (C), respectively.**

| Profile | Scheme | | | | | | | |
|---|---|---|---|---|---|---|---|---|
| | QMF2 | FLMF2 | SLMF2 | RK4MF2 | RK6MF2 | UQ | UFL | USL |
| Simulation results at t = 1000 | | | | | | | | |
| A | 0.85 | 0.87 | 0.72 | 0.87 | 0.99 | 0.38 | 0.97 | 0.97 |
| C | 0.88 | 0.91 | 0.74 | 0.91 | 0.98 | 0.38 | 0.97 | 0.95 |
| D | 0.85 | 0.75 | 0.76 | 0.75 | 0.70 | 0.22 | 0.93 | 0.93 |
| Simulation results at t = 2000 | | | | | | | | |
| A | 0.23 | 0.53 | 0.56 | 0.75 | 0.99 | 0.12 | 0.97 | 0.96 |
| C | 0.15 | 0.92 | 0.60 | 0.82 | 0.98 | 0.02 | 0.96 | 0.93 |
| D | -0.11 | 0.48 | 0.78 | 0.51 | 0.79 | -0.32 | 0.93 | 0.92 |

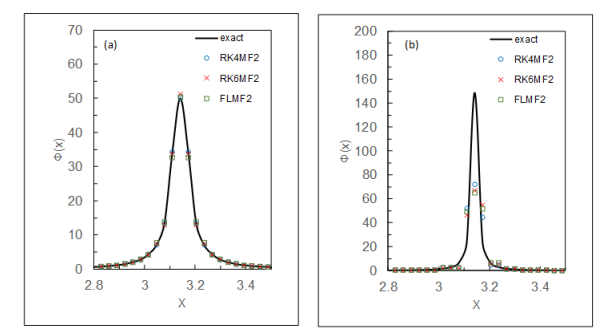


**Figure 5. Simulation results for equation (4) using RK4MF2, RK6MF2 and FLMF2 with Δ= 2π/200 at t = 4(a) and t = 5(b).**

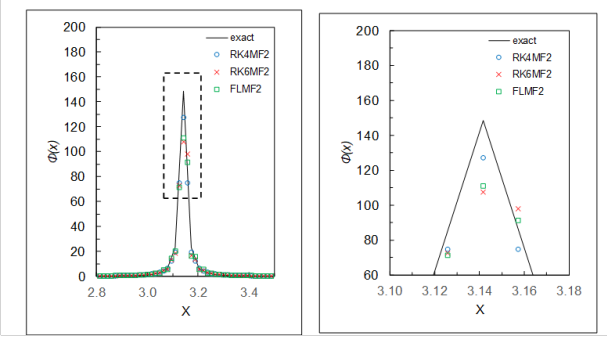


**Figure 6. Simulation results of equation (9) using RK4MF2, RK6MF2 and FLMF2 with Δ= 2π/400 at t = 5.**

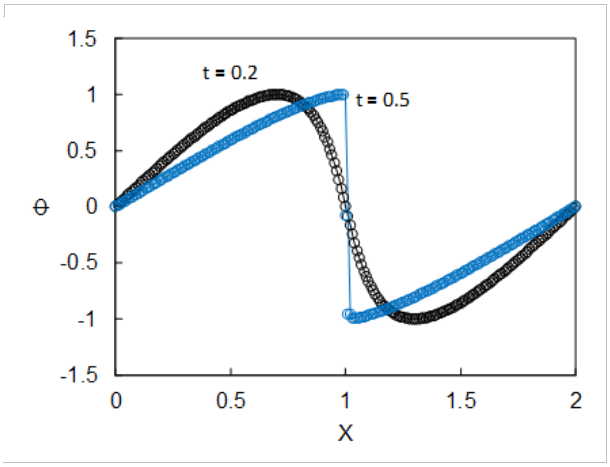


**Figure 7. Solution of Burger Eq. (11) using RK4MF2 Δx = 2/80 at t = 0.2 and 0.5, respectively.**

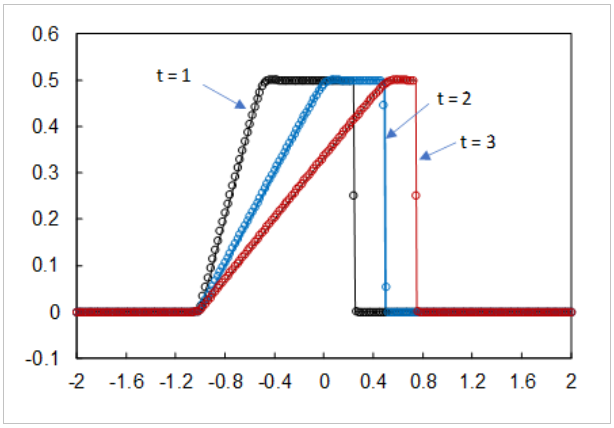


**Figure 8. Solution of Burger equation (11) with initial condition Eq. (12) using RK4MF2 with Δx = 2/100 at t = 1, 2 and 3, respectively**

pattern curve, i.e., initial profile, can be captured well by the numerical model. The NSE value close to 1 indicates that the simulation results are very satisfactory with the initial profile well captured. The NSE values from the simulation results for the schemes reviewed are given in **Table 1**. From **Table 1**, it is seen that the RK6MF2 produces reasonably good results to advection of Gaussian and triangle profiles, with a NSE value above 0.90. The simulation results show that using the modified TVD filter algorithm 2.2 can effectively reduce oscillations and reduce the peak clipping effect if combined with a high-order scheme.

### 4.2 Test 2. (one dimensional equation with variable coefficient). Consider transport equation defined by Eq. (9)

$$\frac{\partial \emptyset}{\partial t} + \frac{\partial}{\partial x}(sin(x)\emptyset) = 0 \quad , 0 \leq x \leq 2\pi \tag{9}$$

The initial condition is φ(x, 0) = 1 and the boundary condition is periodic. The exact solution is (Christlieb et al., 2019)

$$\emptyset(x,t) = sin[2\,tan^{-1}(e^{-t}\,tan(x/2)]/sin(x) \tag{10}$$



Diterima 7 Juli 2022, Direvisi 28 Juli 2022, Diterima untuk dipublikasikan 11 Agustus 2022

In this test case, when time evolves, the mass moves towards the point x = π and forms a profile with a sharp gradient. In this test, we only consider RK4MF2, RK6MF2 dan FLMF2 schemes. **Figure 5** shows simulation results at t = 4 and 5 with 200 spatial grid points. Simulations at t = 4 for the schemes considered produced accurate solutions with the same numerical profiles as the analytical ones. However, simulation results at t = 5 were not very satisfactory. The results will improve by reducing the grid spacing. It can be seen in **Figure 6**, showing the comparison between analytical and numerical solutions at t = 5 using a grid spacing of 400 for RK4MF2, RK5MF2, and FLMF2,

### 4.3 Test 3. (inviscid burger equation).

In this test case we consider a nonlinear scalar defined as **Equation (11)**.

$$\frac{\partial \emptyset}{\partial t} + \frac{\partial}{\partial x}\left(\frac{\emptyset^2}{2}\right) = 0 \tag{11}$$

with initial condition Φ(x,0) = sin(2πx) for 0 ≤ x ≤ 1 and boundary condition

Φ(0,t) = Φ(1,t) = 0. Exact solution is given by Φ(x,t) = sin(x - Φt).

In this case test, the initial profile will evolve and form a steep gradient with time marching around x = 1. The simulation results are only given for the RK4MF2 scheme. **Figure 7** shows the simulation results at t = 0.2 and 0.5 with grid spacing Δx = 2/80. It is seen that the RK4MF2 can give very accurate results and can capture discontinuities without any spurious oscillations, respectively.

Δx = 2/100 at t = 0.2 and 0.5, respectively.

### 4.4 Test 4. (inviscid burger equation.).

This test uses the **Equation (11)** with an initial value consisting of discontinuity defined as

$$\emptyset(x,0) = \begin{cases} 0, & x, -1; \\ \frac{1}{2}, & -1 \le x < 0 \\ 0, & x \ge 0 \end{cases} \tag{12}$$

The exact solution of this problem is defined as (Gao et al., 2012)

$$\emptyset(x,t) = \begin{cases} 0, & x < -1; \\ \frac{x+1}{t}, & -1 \le x < \frac{t}{2} - 1; \\ \frac{1}{2}, & \frac{t}{2} - 1 \le x < \frac{t}{4}; \\ 0, & x \ge \frac{t}{4} \end{cases} \tag{13}$$

The solution can form expansion and shock for t ≤ 4. Calculations were carried out for a grid of 100 cells. The simulation results at three selected times t = 1, 2, and 3 are very satisfactory, as shown in **Figure 8**. It indicates that the modified TVD filter works well for this test

### 4.5 Test 5: (Advection-diffusion equation with variable velocity and dispersion).

Consider advection-diffusion equation defined as

$$\frac{\partial \emptyset}{\partial t} = \frac{\partial}{\partial x}\left[D_o f_1(x,t)\frac{\partial \emptyset}{\partial x} - U_o f_2(x,t)\emptyset\right] \quad 0 \le x \le L \tag{14}$$

where

$$f_1(x,t) = (1 + ax)^2 \quad \text{and} \quad f_2(x,t) = (1 + ax)$$

Initial and boundary conditions are

$$\emptyset(x,0) = 0, \qquad \emptyset(0,t) = 10$$

$$and \ \frac{\partial \emptyset}{\partial x} = 0 \ for \ x \to \infty \ and \ t > 0$$

Analytical solution to this problem was given by Kumar et al. (2010).i.e.

$$\emptyset(x,t) = \frac{\emptyset_o}{2}\left[(1+ax)^{-1} erfc\left\{\frac{ln(1+ax)}{2a\sqrt{D_o t}} - \beta\sqrt{t}\right\} + (1+ax)^{\delta} erfc\left\{\frac{ln(1+ax)}{2a\sqrt{D_o t}} + \beta\sqrt{t}\right\}\right] \tag{15}$$

Where

$$w_o = (au_o - a^2 D_o), \qquad \beta = \sqrt{\frac{w_o^2}{4a^2 D_o} + au_o} = \frac{u_o + aD_o}{2\sqrt{D_o}}, and \ \delta = \frac{u_o}{aD_o}$$

Consider the cases L = 1, $U_o$ = 1, $D_o$ = 0.5 and a = -1. The velocity decreases in the positive x-direction starting from 1 to 0 at x = 1. The mass will accumulate at the end of the channel. The concentration at the end part of the channel, at a reach around x = 1, increases sharply. Simulations were carried out for grid cells 100 and $C_r = u_o\Delta t/\Delta x$ = 0.4 using the splitting method (Holly and Usseqlio-Polatera, 1984) with the convection part solved by the RK4MF2 . The comparison between the numerical and analytical solutions at t = 2 and 4 is given in **Figure 9**. It is seen that RK4MF2 produces accurate solutions where the analytical and numerical solution profiles coincide.

### 4.6 Test 6: Two-dimensional pure convection in rotating fluid

This test considered is pure advection of three solid bodies for a rotating fluid around a square of a side length of 1. This fluid flow field can be viewed as the rotation of a solid body about its center point at the position (0.5,0.5). This case was also studied by Christlieb et al. (2019) and Zhang et al. (2021), The three solid bodies consist of a slotted cylinder, a cone, and a sinusoidal hump. For given $(x_o,y_o)$ let

$$r(x,y) = \sqrt{(x-x_o)^2 + (y-y_o)^2}/0.15$$

The slotted cylinder is defined by

$$\emptyset(x,y,0) = \begin{cases} 1 \ if \ r(x,y) \le 1, \ |x - x_o| \\ 0 \end{cases}$$

$$\ge 0.0225 \ or \ y \ge 0.85 \\ otherwise \tag{16}$$



Diterima 7 Juli 2022, Direvisi 28 Juli 2022, Diterima untuk dipublikasikan 11 Agustus 2022

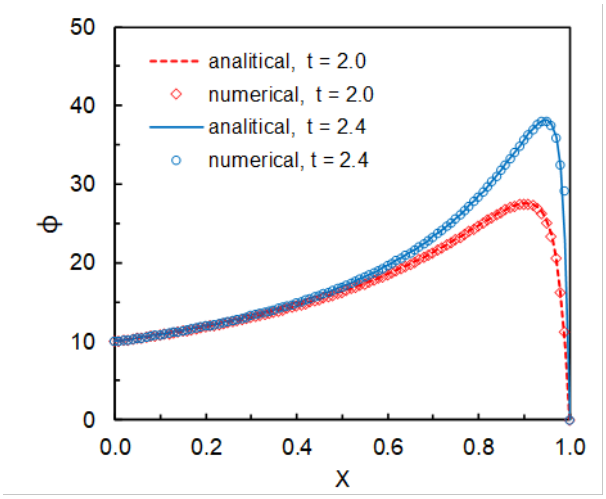


**Figure 9. Simulation results of Advection -diffusion with variable velocity Eq. (14) using RK4MF2 at t = 2 (red diamond) and t = 2.4 (blue circle).**

with its center at $(x_o,y_o) = (0.5,0.75)$.

The center of hump is $(x_o,y_o) = (0.25,0.5)$ and

$$\emptyset(x,y,0) = \frac{1}{4}\{1 + cos[\pi \min(r(x,y),1)]\} \qquad (17)$$

And the cone is described by $(x_o,y_o) = (0.5,0.5)$ and

$$\emptyset(x,y,0) = 1 - r(x,y) \qquad (18)$$

The computational domain is divided into 100x100 grid squares of equal spacing in these simulations. The fluid rotates clockwise at an angular velocity of one

The computational domain is divided into 100x100 grid squares of equal spacing in these simulations. The fluid rotates clockwise at an angular velocity of one complete revolution in 800-time steps. When the diffusion terms are not considered, the solid body should ideally return to its starting point after one revolution without changing shape.

The five schemes, namely QMF2, FLMF2, SLMF2, RK4MF2, and RK6MF2, are reviewed. The plot results of simulation after one rotation are shown in **Figure 10**, with slides profiles of numerical solutions

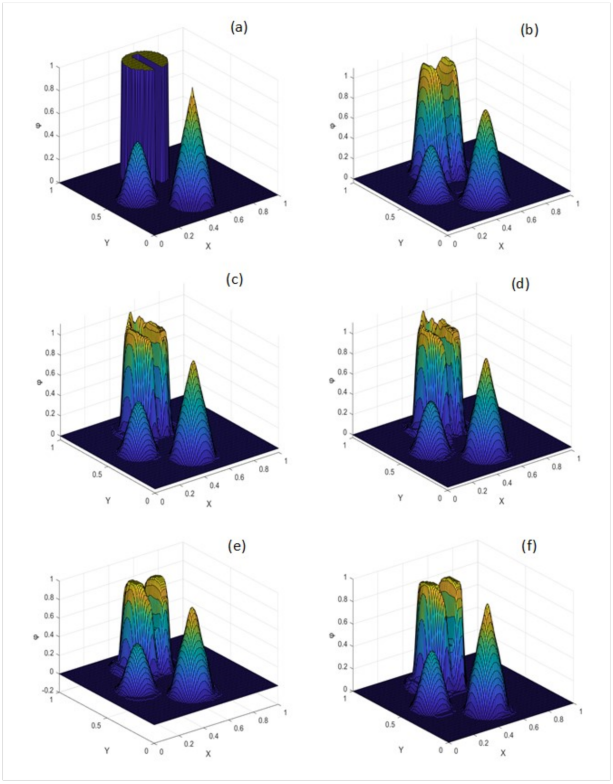


**Figure 10. The plot of initial profile (a) and numerical solutions of rotating three solid bodies problem with 800-time step per rotation, grid mesh 100x100 after completing 1st rotation for (b). QMF2, (c). FLMF2, (d). SLMF2, (e.). RK4MF2, and (f). RK6MF2, respectively**

given in **Figure 11**. The corresponding results after ten cycles are also given in **Figures 12** and **13**. The simulation results show that applying the modified TVD filter algorithm 2.2 to the schemes considered produced no-oscillation solutions. The simulation results at ten rotations show that only the higher-order schemes, FLMF2, SLMF2, RK4MF2, and RK6MF2, can only produce reasonably accurate results for cone and hump profiles with a small clipping effect observed at the extremum. However, all schemes considered cannot capture the slotted cylinder profile adequately.

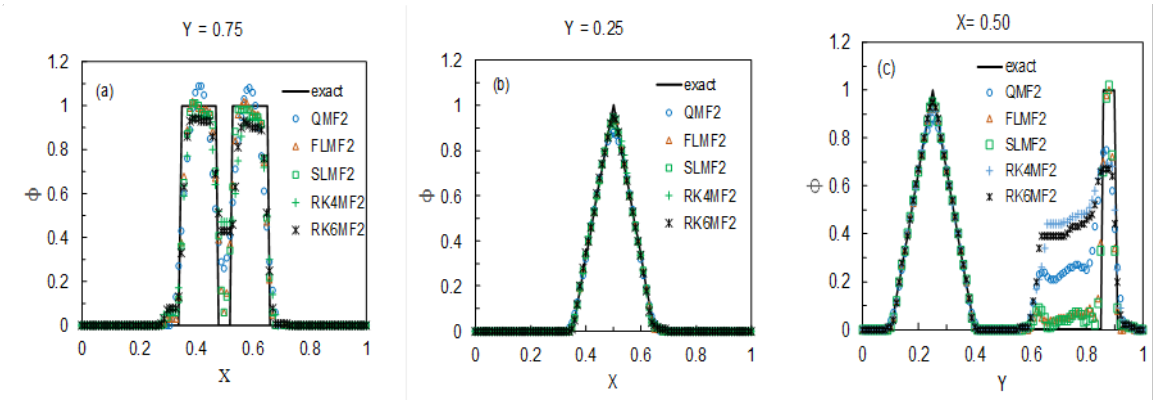


**Figure 11. The plot of the1-D slice of numerical solution of rotating three solid bodies problem at y = 0.75 (a), x = 0.25 (b) and x = 0.50 (c) with 800-time step per rotation, grid mesh 100x100 after completing 1st rotation.**



Diterima 7 Juli 2022, Direvisi 28 Juli 2022, Diterima untuk dipublikasikan 11 Agustus 2022

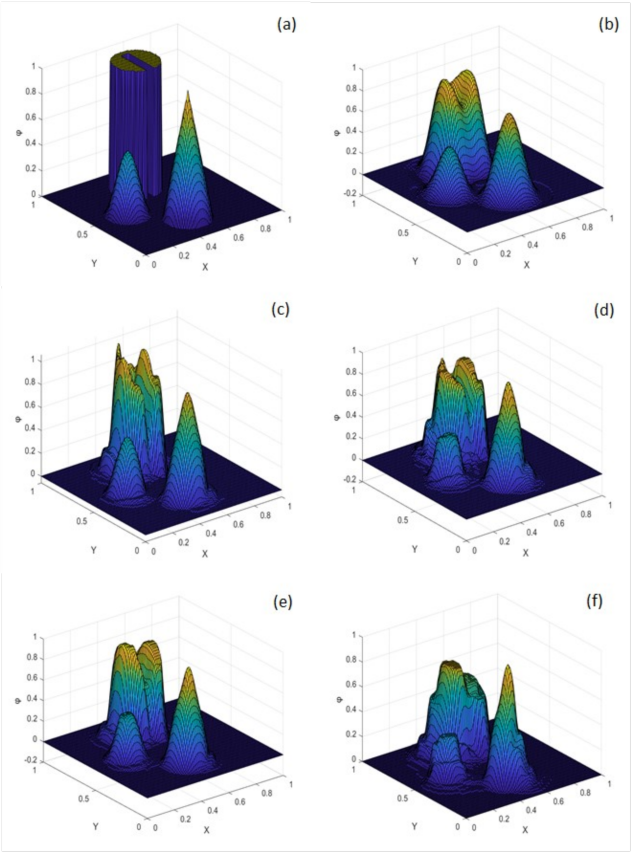


**Figure 12. The plot of initial profile (a) and numerical solutions of rotating three solid bodies problem with 800-time step per rotation, grid mesh 100x100 after completing 10th rotation for (b). QMF2, (c). FLMF2, (d). SLMF2, (e.). RK4MF2, and (f). RK6MF2, respectively.**

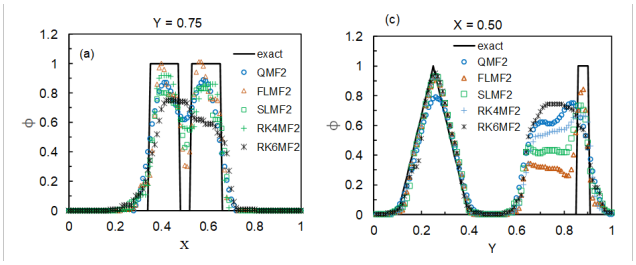


**Figure 13. The plot of the1-D slice of numerical solution of rotating three solid bodies problem at y=0.75 and x = 0.50 with 800-time step per rotation, grid mesh 100x100 after completing 10th t rotation.**

## 4.7 Two-dimensional advection-diffusion with steep inlet profile in rotating flow

This problem is also studied by Smith and Hutton (1982) and Thije Boonkkamp and Anthonissen, (2011 ) defined by **Equation (19)**.

$$\frac{\partial \emptyset}{\partial t}+\frac{\partial (u\emptyset)}{\partial x}+\frac{\partial (v\emptyset)}{\partial y}=\frac{1}{P_e}\left(\frac{\partial^2 \emptyset}{\partial x^2}+\frac{\partial^2 \emptyset}{\partial y^2}\right) \qquad (19)$$

in a rectangular region -1 ≤x ≤1, 0 ≤y ≤1,

where

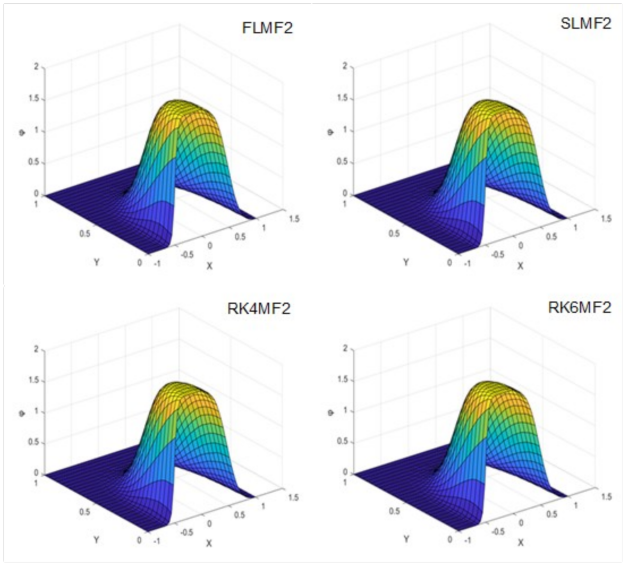


**Figure 14. The plot of numerical solutions of Eq. (19) with grid mesh 25x50 for FLMF2, SLMF2, RK4MF2, and RK6MF2, respectively.**

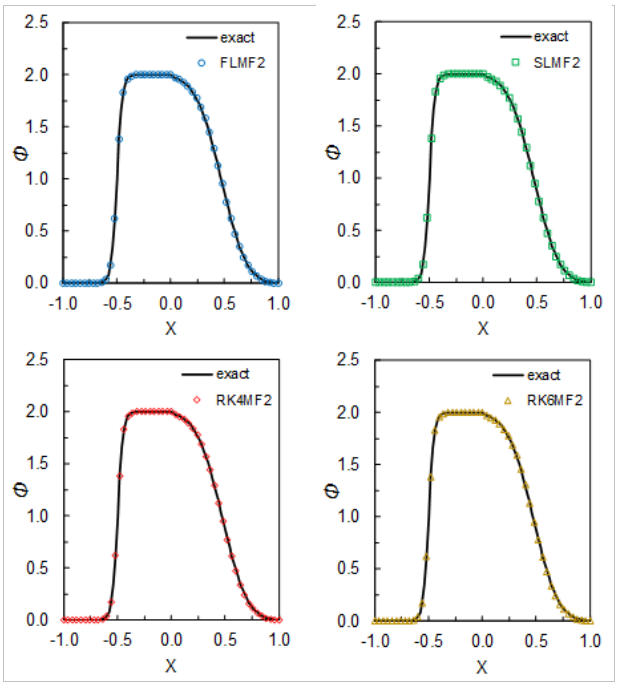


**Figure 15. The plot of the1-D profile of numerical solution Eq. (19) at y = 0 for FLMF2, SLMF2, RK4MF2 and RK6MF2, respectively**

$u(x,y)=2y(1-x^2)$ *and* $v(x,y)=-2x(1-y^2)$

With initial and boundary conditions given by

$\emptyset(x,0)=1+\tanh\big(\alpha(2x+1)\big), -1 \le x \le 0$ (inlet),

$\emptyset(x,y)=1-\tanh(\alpha), (x=\pm 1, 0\le y\le 1)$

*and* $(-1\le x\le 1, y=1)$

$\frac{\partial \emptyset}{\partial y}(x,0)=0, \quad 0\le x\le 1$ $(outlet)$



Diterima 7 Juli 2022, Direvisi 28 Juli 2022, Diterima untuk dipublikasikan 11 Agustus 2022

The problem is actually set as a steady-state one, but it is solved as an unsteady problem so that a steady-state is approached at $t \rightarrow \infty$. Using $\Delta x = \Delta y = 1/25$ and $P_e = 100$, simulations were carried out using an optimal operator splitting proposed by Abarbanel and Gottlieb (1981). The two-dimensional advection-diffusion problem **Eq. (19)** was solved in this splitting technique by consecutive one-dimensional convection and diffusion problems. Then, the advection parts and diffusion parts were computed using the most appropriate schemes. In this test, we consider FLMF2, SLFM2, RK4MF2, and RK6MF2 for solving the 1-D advection in the x and y-directions, respectively, and applying an implicit Crank-Nicholson method for solving the one-dimension diffusion problems in the x and y-directions, respectively. The exact solution was provided by simulation using the ULTIMATE QUICKEST scheme (Leonard, 1988, 1991) on a fine grid of $\Delta x = \Delta y = 1/50$ . Comparisons of the exact and numerical results are shown in **Figures 14** and **15**. The results show that all schemes considered can provide very accurate results with no oscillation found in the solutions.

## 5. Conclusion

The following are some of the findings obtained from the results of this study.

1. Applying non-linear TVD filters algorithm 2.2 proposed by Engquist et al. (1989) to the higher-order finite difference scheme for solving the dominant advection equation can simulate shock or high concentration gradient problems without spurious oscillations. However, the filter has a disadvantage where it flattens true extrema and the scheme reduces to a low order of accuracy locally around true extrema. The numerical exercises show that using the filter for long-term simulation produces inaccurate results.
2. The TVD filter algorithm 2.2 (Cahyono, 2000) was applied in this study to overcome this problem by modifying the admissible1 function to detect the true extremum accurately.
3. Several finite difference schemes have been considered for testing the modified TVD filter algorithm 2.2: Lax-Wendroff, QUICKEST (Leonard,1979), 5th and 6th -order conservative schemes (Leonard, 1988; 1991; Leonard and Mokhtari, 1990), and non-conservative schemes consisting of $5^{th}$ and $6^{th}$ -order Runge-Kutta method. The models have been tested to simulate seven test cases, including a pure advection of scalar profiles, a pure advection with variable velocity, two inviscid burger equations, an advection-diffusion equation with variable velocity and dispersion, advection of three solid bodies in rotating fluid around a square of a side length of 2, and a two-dimensional advection-diffusion equation. The numerical experiments showed that applying the modified TVD filter, combined with the higher-order non-TVD finite difference schemes for solving the advection equation, can produce accurate solutions with no oscillations and no clipping effect extrema.

## References

*Abarbanel, S and Gottlieb, D, "Optimal Time Splitting for Two- and Three-Dimensional Navier-Stokes Equations with Mixed Derivatives", Journal of Computational Physics, vol. 41, (1981) pp. 1-33.*

*Cahyono, M. TVD Filter Algorithm for Solving Advective Transport Equations, Proceeding ITB, (2000), 32,1.*

*Cai, X., Qiu, J. and Qiu, J.M. A conservative semi-Lagrangian HWENO method for the Vlasov equation, Journal of Computational Physics 323 (2016) 95–114, https://doi.org/10.1016/ j.jcp.2016.07.021.*

*Christlieb, A. Guo, W., Jiang, Y., Yang, H., A Moving mesh WENO method based on exponential polynomials for one-dimensional conservation laws, J. Comput. Phys. 380 (2019) 334–354.*

*Deng, X, Shimizu, Y. and Xia, F, A fifth-order shock capturing scheme with two-stage boundary variation diminishing algorithm, Journal of Computational Physics 386 (2019) 323–349.*

*Deng, X.; Shimizu, Y. Xie, B.; Xiao, F. Constructing higher order discontinuity-capturing schemes with upwind-biased interpolations and boundary variation diminishing algorithm. Computers & Fluids. Volume 200, 30 March 2020, 104433*

*Engquist, B., Lotstedt, O., and Sjogreen, B., Nonlinear Filters for Efficient Shock Computation, Mathematics of Computation, Vol.52, No.186, April, (1989), pp.509-537.*

*Gao, W., Li, H., Liu, Y. and Jian, Y.J.,' An oscillation -free high order TVD/CBC-based upwind scheme for convection discretization', Numer Algor (2012) 59:29–50 DOI 10.1007/s11075-011-9474-5.*

*Gaskell, P.H., Lau, A.K.C.: Curvature-compensated convective trasport: SMART, a new boundedness-perserving transport algorithm. Int. J. Numer. Methods Fluids 8, (1988), 617–641.*

*Ha, C. T. and Lee , Jae H. A., A modified monotonicity-preserving high-order scheme with application to computation of multi-phase flows, Computer and Fluids 197 (2020) 104345, https://doi.org/10.1016/ j.compfluid.2019.104345)*



Diterima 7 Juli 2022, Direvisi 28 Juli 2022, Diterima untuk dipublikasikan 11 Agustus 2022

*Holly, F. M and Usseqlio-Polatera, J. M., "Dispersion Simulation in Two-Dimensional Tidal Flow", Journal of Hydraulic Engineering, ASCE, vol. 110, no. 7, July, (1984) pp.905-926, 1984.*

*Huang C, Chen LL. A simple smoothness indicator for the WENO scheme with adaptive order. J. Comput. Phys. 2018; 352:498–515.*

*.Kumar, A., Jaiswal, D.K. and Kumar, N., Analytical Solutions to One-Dimensional Advection-Diffusion Equation with Variable Coefficients in Semi-Infinite Media. Journal of Hydrology, 380, (2010) 330-337. http://dx.doi.org/10.1016/j.jhydrol.2009.11.008*

*Leonard, B.P.: A stable and accurate modelling procedure based on quadratic interpolation. Comput. Methods Appl. Mech. Eng. 19, (1979) 59 –98 (1979)*

*Leonard, B. P, "Universal Limiter for Transient Interpolation Modelling of the Advective Transport Equations, The ULTIMATE Conservative Difference Schemes", Report No: NASA TM-100916 (ICOMP-88-11), NASA Lewis Research, Sep., 1988.*

*Leonard, B. P, "The ULTIMATE Conservative Difference Scheme Applied to Unsteady One-Dimensional Advection", Comput. Methods Appl. Mech. Engrg., 88, (1991) pp. 17-74, 1991.*

*Leonard, B.P. and Mokhtari, S.' ULTRA-SHARP Nonoscillatory Convection Schemes for High-Speed Steady Multidimensional Flow, NASA Technical Memorandum 102568, ICOMP-90-12, April 1990.*

*Leonard, B. P. and Niknafs, H. S., Sharp Monotonic Resolution of Discontinuities Without Clipping of Narrow Extrema, Computer & Fluids, Vol.19, (1991) No.1, pp.141-154.*

*Liu S, Shen Y, Zeng F, Yu M. A new weighting method for improving the WENO-Z scheme. Int. J. Numer. Meth. Fluids (2018);87:271–91.*

*Liu, H., J. Qiu, J.,Finite difference Hermite WENO schemes for conservation laws, II: an alternative approach, J. Sci. Comput. 66 (2016) 598–624.*

*Nash, J. E.; Sutcliffe, J. V. (1970). "River flow forecasting through conceptual models part I — A discussion of principles". Journal of Hydrology. 10 (3): (1970) 282–290. Bibcode:1970JHyd...10..282N. doi:10.1016/0022-1694(70)90255-6.*

*Rodionov, B. V. "Artificial viscosity in Godunov-type schemes to cure the carbuncle phenomenon," J. Comput. Phys. 345, 308–329 (2017). https://doi.org/10.1016/j.jcp.2017.05.024*

*Rajput, U. S. Singh, K. M. A Fifth Order Alternative Mapped WENO Scheme for Nonlinear Hyperbolic Conservation Laws. Adv. Appl. Math. Mech., 14 (2022), pp. 275-298. DOI: 10.4208/aamm.OA-2020-0320*

*Shu, C.W.,Total-Variation-Diminishing Time Discretizations. SIAM Journal on Scientific and Statistical Computation, 9, 1988, 1073-1084. https://doi.org/10.1137/0909073*

*Shu CW, Osher S. Efficient implementation of essentially non-oscillatory shock- -capturing schemes. J. Comput. Phys. 1988;77(2):439–71.*

*Smith, R.M., Hutton, A.G.: The numerical treatment of advection: a performance comparison of current methods. Numer. Heat Transf. 5, (1982) 439–461 (1982)*

*Su Y, Kim S. H. An improved consistent, conservative, non-oscillatory and high order finite difference scheme for variable density low Mach number turbulent flow simulation. J. Comput. Phys. 2018;372:202–19.*

*Thije Boonkkamp, ten, J. H. M., & Anthonissen, M. J. H., The finite volume-complete flux scheme for advection-diffusion-reaction equations. Journal of Scientific Computing, 46(1), (2011), 47-70. DOI: 10.1007/s10915-010- 9388*

*Zhang, H.; Xu, C.; Dong, H. An extended seventh-order compact nonlinear scheme with positivity-preserving. Computer & Fluids. Volume 229, 30 October 2021, 105085*



Diterima 7 Juli 2022, Direvisi 28 Juli 2022, Diterima untuk dipublikasikan 11 Agustus 2022

Diterima 7 Juli 2022, Direvisi 28 Juli 2022, Diterima untuk dipublikasikan 11 Agustus 2022